A High-Accuracy, Calibration-Free Technique for Measuring the Electrical Conductivity of Molten Oxides

SUSAN L. SCHIEFELBEIN and DONALD R. SADOWAY

A high-accuracy, calibration-free technique to measure the electrical conductivity of molten oxides has been developed—the coaxial cylinders technique. Because the melt under investigation comes in contact only with metal and not with anything dielectric, the new technique enables the measurement of the electrical properties of liquids inaccessible by classical high-accuracy techniques. Two coaxial cylindrical electrodes are immersed in the melt to an arbitrary initial depth, and ac impedance is measured over a wide range of frequency. The electrodes are then immersed deeper, and ac impedance is again measured over the same range of frequency. This process is repeated at multiple immersions. The electrical conductivity is calculated from the change in measured conductance with immersion. The temperature dependence of electrical conductivity has been measured for two oxide melts: (M) 50.95 pct CaO, 12.51 pct MgO, 36.54 pct SiO_2, 1733 K $< T <$ 1843 K; and (S) 24.59 pct CaO, 26.15 pct MgO, 49.26 pct SiO_2, 1763 K $< T <$ 1903 K, where concentration is expressed in mole percent. Both melts exhibited behavior characteristic of ionic liquids.

I. INTRODUCTION

AS part of a larger study of the physical chemistry of molten oxides for use as electrolytes in prospective high-temperature electrochemical processes such as electrolytic steelmaking,[1,2] the electrical conductivities of multicomponent molten oxides were investigated. In order to support the electrolysis of iron oxide to produce pure liquid iron and oxygen gas, for example, a melt must

(1) be an ionic conductor;
(2) have an acceptable value of electrical conductivity, i.e., one that satisfies the thermal needs of the electrolysis cell while sustaining economically viable metal production rates;
(3) be free of elements more noble than iron—such elements would codeposit with iron and contaminate the metal product;
(4) have a low vapor pressure;
(5) be less dense than liquid iron—this ensures good separation of metal product from electrolyte;
(6) have a high solubility for iron oxide;
(7) be environmentally benign, and
(8) be low cost.

Melts based on SiO_2 are promising as candidate electrolytes, as many silicates are known to meet the last six criteria. The first two criteria, those concerning the electrical properties of the melt, are the most difficult to assess due to a general lack of data and conflicting information.[15–24] Obtaining reliable data, then, became the focus of the present study. In response to the lack of a fully satisfactory technique for making high-accuracy measurements in the melts of interest, a new technique was developed, the co-axial cylinders technique.[3,4] The purpose of this article is to demonstrate the applicability of the new technique to the measurement of the electrical properties of oxide melts.

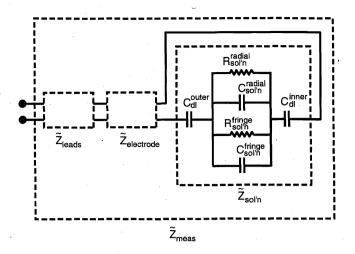## II. REVIEW OF AVAILABLE TECHNIQUES

For the measurement of the electrical conductivity of a liquid, the literature reports 11 techniques based on eight electrode designs. In the opinion of the authors, none is fully capable of supplying high-accuracy data in molten oxide systems. Thus, although the electrical conductivities of various molten oxides have been measured in the past, it is the opinion of the authors that these data are, by and large, inaccurate. For a complete review of these techniques along with an explanation of their shortcomings, the reader is directed to another document.[5] Very briefly, what sets high-accuracy techniques apart from low-accuracy techniques is that high-accuracy techniques establish well-defined current paths, i.e., current paths whose functional dependence upon the electrical properties of (1) the liquid under investigation, (2) the electrodes, and (3) the container is well characterized.

There were seven low-accuracy techniques based on five electrode designs: (1) two wire, (2) four wire, (3) four wire with double immersion, (4) crucible, (5) differential crucible, (6) ring, and (7) two toroid. Low-accuracy techniques have certain advantages and are well suited for particular applications. In general, low-accuracy techniques are less complicated than high-accuracy techniques. For making quick laboratory measurements or monitoring an industrial process stream, a low-accuracy technique is often most appropriate.

There were four high-accuracy techniques based on three electrode designs: (1) interdigitated, (2) capillary, (3) differential capillary, and (4) meandering winding. The suitability of a given technique is governed by the relationship between the range limits of the available impedance measuring instrument and the conductance of the liquid under investigation, i.e., the conductivity as seen through the cell factor of the particular electrode configuration. The inter-

Fig. 1.—Equivalent circuit of coaxial cylinders cell.

$\tilde{Z}_{meas}$: total measured impedance

$\tilde{Z}_{leads}$: leadwire impedance

$\tilde{Z}_{electrode}$: electrode impedance

$\tilde{Z}_{sol'n}$: solution impedance

C_{dl}^{outer} : double-layer capacitance (outer electrode)

C_{dl}^{inner} : double-layer capacitance (inner electrode)

$R_{sol'n}^{radial}$: radial component of solution resistance

$C_{sol'n}^{radial}$: radial component of solution capacitance

$R_{sol'n}^{fringe}$: fringe component of solution resistance

$C_{sol'n}^{fringe}$: fringe component of solution capacitance

digitated electrode design, featuring relatively short and wide current paths, is best suited for use in highly resistive liquids (*e.g.*, transformer oil), while the capillary design, featuring relatively long and narrow current paths, is best suited for use in highly conductive liquids (*e.g.*, molten NaCl). The meandering winding method, which has been used for measuring the electrical conductivity of solid metals, is, in principle, suitable for use with highly conductive liquids.

Since the molten oxides of interest are highly conductive, the interdigitated design was deemed unsuitable. As for the capillary design and the meandering winding method, it was not possible to identify a material that satisfied the requirements for use in molten oxides: to provide a well-defined current path, the material must be dielectric and dimensionally stable; to prevent contamination of the liquid under investigation, the material must be chemically inert.

III. THE NEW TECHNIQUE

Electrical conductivity is an intensive property and cannot be measured directly; it must be calculated from a measurement of the corresponding extensive property, resistance:

$$R = \rho\left(\frac{l}{A}\right) = \left(\frac{1}{\kappa}\right)\left(\frac{l}{A}\right) \qquad [1]$$

where R is resistance, ρ is electrical resistivity, κ is electrical conductivity, l is the length of the current path, and A is the cross-sectional area of the current path. The resistance of the solution as defined in Eq. [1] can be measured by a variety of techniques, both dc, *e.g.*, stepped-potential current decay, and ac, *e.g.*, electrochemical impedance spectroscopy. The latter was used in the present investigation.

In electrochemical impedance spectroscopy, the electrical conductivity of a melt is derived from its impedance, $\tilde{Z}_{sol'n}$ (the tilde denotes a complex number). However, an actual impedance measurement, $\tilde{Z}_{meas}$, necessarily contains contributions from other sources, *i.e.*, electrodes, leadwires, *etc.*, so that $\tilde{Z}_{meas} \neq \tilde{Z}_{sol'n}$. The primary goal of the data reduction procedure is extraction of κ from $\tilde{Z}_{meas}$.*

---

*In this analysis, the electrode is assumed to be equipotential; hence, its resistance can be treated as independent of depth of immersion. When this simplifying assumption does not apply, the electrode must be modeled as a transmission line, and a much more complicated analysis must be employed to extract κ from $\tilde{Z}_{meas}$.[5]

The equivalent circuit for the measurement is shown in Figure 1. Summing series impedances gives

$$\tilde{Z}_{meas} = \tilde{Z}_{leads} + \tilde{Z}_{electrode} + \tilde{Z}_{sol'n} \qquad [2]$$

where $\tilde{Z}_{leads}$ is the impedance of the leadwires from the impedance measuring instrument, $\tilde{Z}_{electrode}$ is the impedance of the electrodes, and $\tilde{Z}_{sol'n}$ is the impedance of the solution under investigation. Since κ derives solely from $\tilde{Z}_{sol'n}$, $\tilde{Z}_{leads}$ and $\tilde{Z}_{electrode}$ must be eliminated from $\tilde{Z}_{meas}$. This is done by measuring the impedance of the system with the electrodes shorted, then subtracting this from $\tilde{Z}_{meas}$.* As κ influences

---

*Being predominantly inductive, $\tilde{Z}_{leads}$ is extremely sensitive to configuration and placement of the leadwires. It is therefore essential that the position of the leadwires be strictly fixed throughout the course of the measurement procedure. In addition, Kelvin connections should be employed with the voltage sense leads tied to the current supply leads at the top of the electrodes.

---

only resistance (not capacitance or inductance), it is necessary to isolate the *purely resistive* part of $\tilde{Z}_{sol'n}$, denoted here as $(Z_{sol'n}^{real})^*$.

In brief, the procedure for obtaining κ from $\tilde{Z}_{meas}$ consists of the following steps when coaxial cylinder electrodes are used.

(1) Impedance measurements are taken over a wide frequency range at many successive depths of immersion.
(2) Using a short circuit correction, $\tilde{Z}_{sol'n}$ at each immersion is isolated from $\tilde{Z}_{meas}$.
(3) The value of $(Z_{sol'n}^{real})^*$ at each immersion is found by choosing the value of $Z_{sol'n}^{real}$ at which $(-Z_{sol'n}^{im})$ is a minimum.
(4) $1/(Z_{sol'n}^{real})^*$ is plotted *vs* the corresponding relative immersion, ξ.
(5) The slope of this straight line, $[d(1/(Z_{sol'n}^{real})^*)]/d\xi$, is multiplied by the constant, $[\ln(b/a)]/2\pi$, to yield the electrical conductivity of the solution, κ.[25] The variables a and b represent the diameters of the inner and outer electrodes, respectively, as depicted in Figure 5.

In addition to its unique capability of making high-accuracy measurements in oxide melts, the new technique has attributes that make it attractive for use in other types of
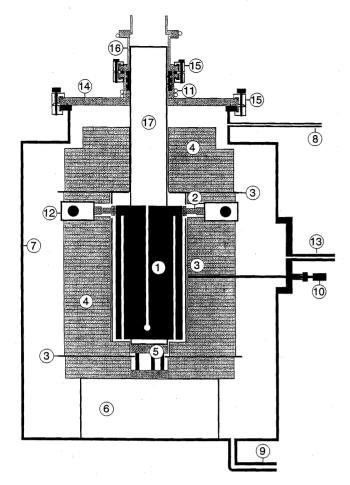
Fig. 2.—Cross section of the high-temperature furnace.

① graphite heater
② tungsten studs
③ Mo radiation shields
④ graphite felt insulation
⑤ Mo pedestal
⑥ stainless steel platform
⑦ stainless steel shell
⑧ gas outlet
⑨ gas inlet

⑩ control thermocouple
⑪ Cu water cooling tubes
⑫ water-cooled power lead
⑬ vacuum connection
⑭ furnace lid
⑮ clamps
⑯ water-cooled feedthrough
⑰ COE Al_2O_3 reaction tube

liquids. Because the constant $[\ln (b/a)]/2\pi$ is calculated directly from electrode geometry, the coaxial cylinders technique does not require calibration in a standard reference liquid. This is arguably the greatest advantage of the new technique. Furthermore, it is necessary to know only the *relative*, not the *absolute*, position of the electrodes. This feature is most advantageous in "blind" experiments such as those conducted at high temperatures in a furnace. As well, this feature is useful even when the solution and electrodes are in clear view, because wicking and other surface effects make it difficult, if not impossible, to determine absolute immersion.

For a more detailed description of the technique, the reader is directed to another document.[5]

Certification in Aqueous Solutions

Electrical conductivity measurements of KCl (aq) reference solutions spanning three decades of concentration yielded results deviating by less than ±0.5 pct from the accepted standard values.[5] This certified the electrode design, experimental procedure, attendant data analysis, and proposed equivalent circuit. In addition, these measurements in aqueous solutions provided confirmation of theories concerning placement of the electrodes relative to the container walls and floor.

IV. ELECTRICAL CONDUCTIVITY MEASUREMENTS OF MOLTEN OXIDES

The electrical conductivities of two oxide melts, M and S, were measured as a function of temperature. The term "S" denotes the composition richer in silica, and "M" denotes the composition richer in metal-oxide modifier. Both melts exhibited Arrhenius behavior: electrical conductivity increased with temperature, and ln (κ) varied linearly with ($1/T$). This, in conjunction with the derived values of the activation energy for electrical conduction, E_κ, indicated that the melts were ionic. Furthermore, as expected, E_κ of melt S was greater than E_κ of melt M. These results demonstrate the utility of the coaxial cylinders technique in molten oxides.

A. EXPERIMENTAL APPARATUS

1. Furnace

A cross section of the furnace is shown in Figure 2. A water-cooled feedthrough, designed and fabricated for this project, provides a gas-tight seal between the furnace chamber and the closed-one-end (COE) alumina reaction tube. The gas atmosphere for the experiment in the reaction tube is separate from both the furnace atmosphere and the laboratory atmosphere and, thus, can be varied independently.

The furnace can easily reach 1800 °C and has a vertical isothermal zone ~1-in. long, where the temperature deviates less than ±5 °C at 1500 °C. The cylindrical "birdcage" type heater was machined from premium-grade graphite rod (Grade ATJ, Union Carbide, Chicago, IL) and was electrically connected to water-cooled copper current feeds *via* studs. The heater was insulated by one cylindrical molybdenum radiation shield surrounded radially by about 3 in. of graphite felt insulation. Additional sheets of molybdenum and layers of graphite felt were positioned above and below the heater.

The furnace chamber had to be oxygen free to prevent oxidation of the graphite heater. This was accomplished at lower temperatures by evacuating the chamber to 40 mTorr (mT) by means of a rotary vane mechanical pump, and at higher temperatures by flowing ultra-high-purity (UHP) argon gas (grade 5.0) through the chamber.

2. Motion apparatus

Figure 3 shows the device, based on metal bellows, used to vertically translate the electrodes without disturbing the inert atmosphere required for these high-temperature experiments. The bellows are extended or compressed by turning the nuts. The nuts engage rods, attached to the top bellows fitting, which extend outside the threaded aluminum tube through vertical slits. The vertical distance traversed is precisely measured by a digital micrometer mounted on the threaded aluminum tube. Figure 4 shows how the bellows device fits onto the furnace *via* specially

made water-cooled fixtures. Alignment and electrical iso-lation of the electrode leads and thermocouples were ac-complished by way of a custom vacuum-tight feedthrough, which serves as the lid for the bellows structure. The place-ment of the feedthrough is shown in Figure 3.

3. Electrode

Electrode assemblies able to survive the high tempera-tures and the severe environment of molten oxides were designed and constructed. Due to its chemical resistance to silicates and its machinability, molybdenum was used for all parts that would contact the liquid.

Figure 5 shows the high-temperature electrode assembly. The outer electrode was machined from a solid rod, 1.25-in. diameter (Schwarzkopf Development Corp., Holliston, MA). The inner electrode and all electrode leads were straight molybdenum rods, 0.125-in. diameter. The screw connector, used to precisely position the inner electrode co-axial with the outer electrode, was made of boron nitride (BN) (HBC grade, Union Carbide, Chicago, IL). The BN connector had several small-diameter, vertical through-holes to permit the gas flow required when raising or low-ering the electrodes in the melt. The two leads to the outer electrode, current supply and voltage sense, were threaded and screwed into place along diameter X—X in Figure 5. The inner electrode itself served as its own current supply lead. The voltage sense lead to the inner electrode was con-nected via a molybdenum bar along section Y—Y in Figure 5. Several BN heat shields (disks) were fitted on the leads a few inches above the top of the electrode to reduce heat loss and to improve alignment and stability of the entire electrode assembly.

4. Certification

In order to certify the high-temperature apparatus, it was used to measure the electrical conductivity of 1.0 D KCl (aq)* at room temperature. The entire apparatus, i.e., mo-

---

*The demal (D) is a concentration unit used in connection with the electrical conductivity of aqueous solutions and is defined as follows: a 1 D solution consists of 71.1352 g KCl per kg solution, a 0.1 D solution consists of 7.41913 g KCl per kg solution, and a 0.01 D solution consists of 0.745263 g KCl per kg solution.

---

lybdenum electrode assembly, molybdenum crucible, mo-tion apparatus, and furnace (power off), was put into ser-vice to make this measurement. The procedure was identical to that used previously to certify the original ap-paratus built for ambient temperature service.[5] The high-temperature apparatus measured a value of 0.1043 S cm^{-1} at 21.5 °C, which is within ±0.2 pct of the standard ref-erence value, 0.1045 S cm^{-1}.[6,7]

B. Oxide Compositions

The system CaO-MgO-SiO$_2$ was chosen for this study because it is one of the simplest systems (i.e., contains the fewest components) that satisfies all the physicochemical requirements of direct oxide electrolysis (Section I) and al-lows significant variation in composition at temperatures below 1600 °C. The 1400 °C and 1600 °C liquidus lines, as well as the specific compositions chosen for this study, are shown on the ternary phase diagram (Figure 6), which has been reproduced here for the convenience of the reader.[3]
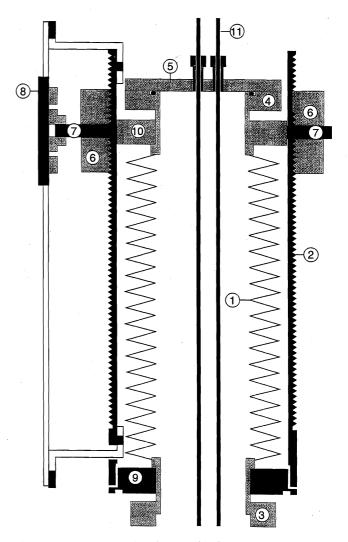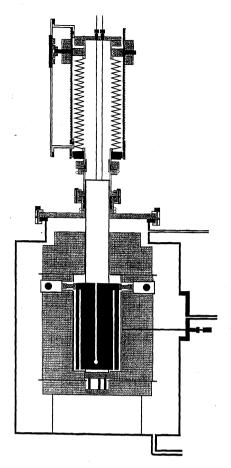

Fig. 3.—Motion apparatus based on metal bellows.

① metal bellows   ⑥ nuts
② threaded Al tube   ⑦ rods
③ bottom bellows fitting   ⑧ digital micrometer
   (to furnace)   ⑨ bottom connector
④ top bellows fitting   ⑩ top connector
⑤ feedthrough   ⑪ electrode assembly (simplified)

The compositions (in mole percent) of the two melts in this study are as follows: (M) 50.95 pct CaO, 12.51 pct MgO, 36.54 pct SiO$_2$; and (S) 24.59 pct CaO, 26.15 pct MgO, 49.26 pct SiO$_2$.

The choice of compositions can be explained with ref-erence to the relevant melt structure. The structure of liquid silicates varies widely with silica content, and electrical conductivity is known to depend on liquid structure.[8,9] In general, molten silicates consist of three-dimensional inter-connected networks of SiO$_4^{4-}$ tetrahedra in which silicons are joined by bridging oxygen atoms.[10,11] The gradual ad-dition of basic oxides (e.g., CaO) results in the progressive breaking of these oxygen bonds with the formation of non-bridging oxygens, and eventually the formation of free ox-ygen ions.[8]

Melts high in silica (acidic melts) consist of a silica net-work in which there are no free oxygen ions—all oxygens are bound to either one or two silicons. In the acid limit

Fig. 4.—Motion apparatus, electrode assembly, and furnace used in high-temperature experiments.

dielectric material

Mo connector

Fig. 5.—High-temperature electrode.

● melt S
● melt M
— 1400°C liquidus
■ ■ ■ 1600°C liquidus
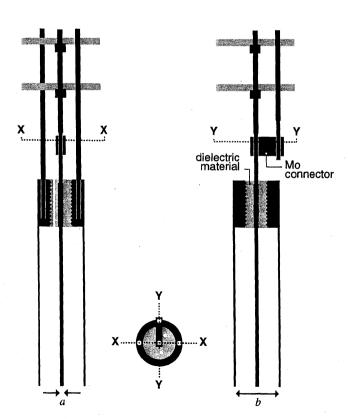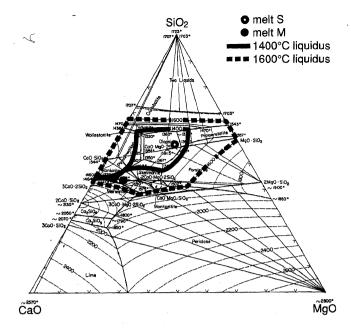
Fig. 6.—Pertinent liquidus lines and compositions in the ternary system CaO-MgO-SiO$_2$.

(pure silica), the liquid is completely networked and contains no free oxygen anions. In the basic limit, the silica network is completely broken, and silica is present only as the orthosilicate, SiO_4^{4-}.

Compositions M and S were chosen because they have different structures. Composition M is near the orthosilicate composition, the border between acidic and basic melts. This melt should have little to no network structure. Silica should be present as the orthosilicate, and the melt may contain some free oxygen ions. Composition S, on the other hand, being a somewhat acidic melt, should possess some network structure and contain very few free oxygen ions.

Melt preparation

High-purity oxide powders* were weighed and mixed,

then premelted in large, high-density MgO crucibles (Ozark Technical Ceramics, Webb City, MO) in an induction furnace open to the atmosphere.** Premelting was necessary

because the ratio of powder volume to liquid volume is greater than 4. Premelting in MgO crucibles required the master compositions to be at MgO saturation; however, actual electrical conductivity measurements were made in molybdenum crucibles, and so compositions were not limited to MgO saturation. For example, the S composition was produced by charging SiO$_2$ powder along with a premelted master composition in the molybdenum crucible used for the conductivity measurement. The cooled premelted oxides were carefully separated from the MgO crucible and then crushed between molybdenum plates in a hydraulic press. The bright white appearance of the crushed oxides was evidence of their high purity. Chemical analyses

(DCP analysis, Allegheny Ludlum Corp., Brackenridge, PA) confirmed the compositions.

C. EXPERIMENTAL PROCEDURE

1. Preliminaries

Prior to use at high temperatures, all molybdenum parts (crucible, electrode, *etc.*) were thoroughly cleaned and dried, and all BN parts were given appropriate heat treatments (Appendix A provides details).

The electrodes and leads were then carefully assembled. Cotton gloves were worn at all times to avoid contaminating the electrodes with natural oils. Once the proper coaxial placement of the inner electrode was verified (by way of an aluminum foil impression), the four leads of the electrode assembly were secured in the top fitting lid. Two type-C thermocouples in molybdenum sheaths were then added to the top fitting, fed through the BN heat shields, and aligned with the bottom of the electrodes—one was positioned 0.25 in. above, and one 0.25 in. below. All leads and thermocouple sheaths were electrically insulated from the top fitting (and each other) by tight-fitting PTFE sleeves. Finally, a 0.125-in. molybdenum rod for sampling the melt was secured in the top fitting.

With the electrode assembly ready to go, a molybdenum crucible (2-in. o.d., 0.05-in. wall, 5.5-in. tall) was charged with about 300 g of crushed premelted oxide. This amount of premelted oxide resulted in a liquid pool about 3-in. deep. The crucible was positioned centrally in the COE alumina reaction tube. A molybdenum ''fringe collar'' was secured around the crucible diameter to aid centering in the reaction tube. The motion apparatus was then attached to the furnace. Finally, the electrode assembly was lowered through the motion apparatus and the top fitting secured *via* bolts to the O-ring seal.

The reaction chamber was evacuated and backfilled with UHP argon several times. The chamber was then left under vacuum until reaching about 50 mT (one day minimum). Next, the furnace was heated to 400 °C over the course of 2 to 5 days, depending on the condition of the charge. The chamber was left under vacuum at 400 °C until reaching about 50 mT (2 days minimum). The temperature controller was then set to ramp the temperature to ~1500 °C over 12 hours. The heating rate was limited by the alumina reaction tube—maximum 200 °C hr^{-1}.

2. Measurements

The melt surface was located by slowly lowering the electrodes while making an impedance measurement—the impedance dropped precipitously when the electrodes first contacted the melt. The vertical position of the surface was recorded. The electrodes were then slowly immersed into the melt beyond the deepest immersion for impedance measurements (about 2 in.), then slowly raised to an immersion of about 0.5 in. The electrodes were left at the shallow immersion for at least 10 minutes to establish thermal equilibrium.

The electrodes were then lowered to the first immersion, ~0.7 in. After 2 minutes (for thermal equilibrium), the temperature was recorded and impedance measured over the frequency range 350 to 1 kHz.* The electrodes were then

---

*This frequency range was determined in a previous experiment and was chosen to include the critical point in the impedance plane plot. The

instrumentation for making impedance measurements consisted of a waveform generator/response analyzer (Solartron model 1260 Frequency Response Analyzer (Solartron Instruments, Burlington, MA)) controlled by a personal computer using a combination of commercially available software (Z60, Scribner Associates, Inc. (Charlottesville, VA)) and code written in house expressly for this investigation. Additional details regarding the impedance measurements are given in Appendix B.

---

lowered to the next immersion, ~0.05 in deeper, and the process repeated. It is worth noting that the electrodes were always *lowered* to the next immersion—*raising* the electrodes to the next immersion caused reproducibility problems. This was probably the result of the hysteresis in the contact angle of liquid oxides on solid metals—there is often a considerable difference between the angle at which a liquid advances over a solid surface and the angle at which the liquid recedes from a previously wetted surface.[12] This effect was peculiar to the molten silicates—other liquids investigated (molten chlorides, molten nitrates, and aqueous salt solutions) did not exhibit this behavior. Impedance measurements were taken at a minimum of six successive immersions. After the last measurement, the electrodes were slowly raised out of the melt.

The furnace was then ramped to the next temperature of interest. An effort was made to avoid always heating or always cooling between temperatures—the initial measurement was made at an intermediate temperature so that, between measurements, the temperature was sometimes increased and sometimes decreased. The entire process was repeated at a minimum of six temperatures, and several measurements were repeated to check reproducibility. After all measurements at all temperatures were complete, the molybdenum sampling rod was plunged into the melt to obtain a sample for chemical analysis.

The integrity of the experimental apparatus and atmosphere was confirmed by the bright silvery appearance of all molybdenum parts (electrode, crucible, *etc.*) exposed to the high temperatures. In addition, there was no sign of attack by the melt—the lower half of the electrodes that had been immersed in the molten oxide appeared clean, smooth, and lustrous.

In a separate experiment, the electrodes were shorted by shallow immersion in liquid silver saturated with molybdenum. Impedance measurements were made over exactly the same frequency range and at the same increments as for the molten oxides. The impedance data for the oxide melt and the liquid metal short were combined to give values for the electrical conductivity of the oxide melt at each temperature.

D. Results and Discussion

The measured values of electrical conductivity of melts M and S have been fit by least-squares regression to an Arrhenius-type equation. The results are as follows.
For melt M,

$$\ln \kappa = 6.5586 \ (\pm 0.357) - 13{,}262 \ (\pm 639)/T, \\ 1733 < T < 1843$$

For melt S,

$$\ln \kappa = 7.1779 \ (\pm 0.553) - 15{,}892 \ (\pm 1{,}010)/T, \\ 1763 < T < 1903$$

where κ is in S cm^{-1} and T is in Kelvins. The results are plotted in Figure 7.
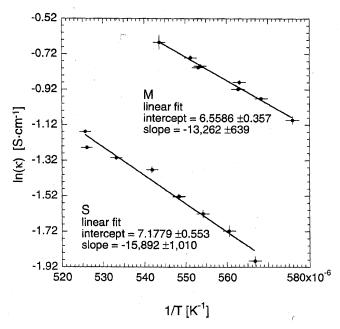
Fig. 7.—Temperature dependence of the electrical conductivities of melts M and S.
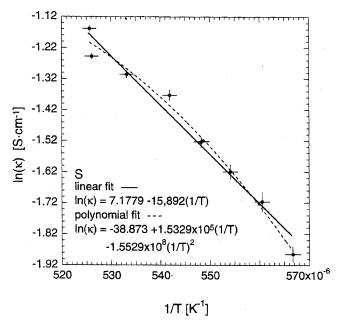

Fig. 8.—Comparison of linear and polynomial fits of data for melt S.

Table I. Comparison of Results of the Present Investigation with Those of Kawahara et al.[14]

Melt Composition	κ (S cm^{-1})	
	This Study	Kawahara et al.
M	0.49	>0.7
S	0.21	~0.45

The activation energy of electrical conduction, E_κ, was calculated to be 110 ± 5 kJ mol^{-1} for composition M and 132 ± 8 kJ mol^{-1} for composition S. These values, in conjunction with the values of κ, suggest that these melts are predominantly ionic.

Although the data for melt S are appropriately modeled

as linear, a polynomial fit was found to be slightly better:

$$\ln \kappa = -38.873 + 1.5329 \times 10^5 \, (1/T) - 1.5529 \times 10^8 \, (1/T)^2$$

as seen in Figure 8. Nothing was gained by a polynomial fit of the data for melt M. Melt S is acidic and, therefore, possesses some silicate network structure; melt M is neither acid nor base and, therefore, contains little to no silicate network structure. The slight curvature in the S data may be due to changes in the liquid structure, e.g., breaking up of the polymer network with increased temperature (thermally induced chain scission).[13] The degree of polymerization influences electrical conductivity. The greater the average chain length in the network, the greater the barrier to the movement of cations through the melt. This is not to suggest that electrical conductivity is directly related to viscosity. Electrical conductivity is predominantly controlled by the movement of the most mobile species (cations in the case of molten silicates), while viscosity is controlled by the movement of the least mobile species (the anionic silicate network in the case of molten silicates).

There is only the study by Kawahara et al.[14] that is directly comparable to the present work. Unfortunately, their results are problematic because they employed the ring technique, which suffers from the fact that the current path is a function of the electrical properties of (1) the liquid under investigation, (2) the electrodes, and (3) the container.[5] Predictably, their values of electrical conductivity do not closely agree with those measured in the present study. Table I compares the results of the two investigations at 1550 °C, the only temperature at which data are reported by Kawahara et al.*

---

*Kawahara et al. report their data at 1550 °C in the form of isoelectrical conductivity lines on the ternary CaO-MgO-SiO$_2$ phase diagram. The values given in Table I were estimated from Fig. 10 in Ref. 14.

ACKNOWLEDGMENTS

APPENDIX A
Molybdenum and Boron Nitride Treatments

A. Molybdenum

All molybdenum parts (electrode, thermocouple sheaths, and crucible) were first mechanically cleaned (with sand-

paper, steel wool, *etc.*) to remove residual grease, then subjected to the following chemical treatment.

1. *Solution A*
(a) Deionized water, 65 mL;
(b) CrO_3, 20 g; and
(c) H_2SO_4, 35 mL.
Mix in the order given; add the acid slowly while stirring.

2. *Solution B*
(a) Tap water, 6 vol;
(b) HNO_3 (concentrated commercial), 13 vol; and
(c) HF (concentrated commercial), 1 vol.
Mix in the order given.

3. *Procedure*
Immerse parts in solution B and rinse briefly in tap water; immerse parts in solution A and agitate for 30 seconds; drain off and rinse immediately in running tap water; boil in fresh deionized water 10 minutes—pour off; rinse in fresh methanol; rinse in fresh acetone; drain as thoroughly as possible and dry in oven not above 80 °C.

Note 1: Discard solution A after it turns green.

Note 2: Molybdenum parts cleaned in this way are silvery bright—if left too long in solution B, the surface may be etched.

Caution 1: Reaction between molybdenum metal and solution B is quite vigorous and potentially explosive—avoid deep immersion of parts for extended periods.

Caution 2: Avoid contact between solution A and organic solvents such as methanol or acetone.

B. *Boron Nitride*

Boron Nitride must be heat treated to remove moisture and binders—without treatment, it is likely to shatter upon initial heating. After use at high temperature, the BN parts must be stored with a desiccant. If significant exposure to air occurs, the heat treatment must be performed again to remove moisture.

Pyrolytic BN: Fire in air (or argon) at 700 °C for 10 hours (no restriction on heating rate); cool to room temperature in flowing argon gas; store in desiccator.

Hot-Pressed BN (HBC grade): In argon atmosphere, heat at 250 °C per hour to 1000 °C; hold for 10 hours at 1000 °C; cool to room temperature in flowing argon gas; store in desiccator.

APPENDIX B
1260 FRA Settings

The Solartron 1260 FRA was run in current control mode* and was controlled by a personal computer using

*Current control is recommended by the manufacturer for measurement of impedance less than 50 Ω.

Z60 software (Scribner Associates, Inc., Charlottesville, VA) with the following settings.

A. *Analyzer*

Auto integration type: off
Measurement integration time: 0.5 s
Measurement delay time: 5 cycles
Mode: impedance; null file: [none]
Source: V1/*i*
Range input V1: 30 mV
Range input V2: [none]
Range input *i*: 60 mA
Coupling input V1: dc
Coupling input V2: dc
Coupling input *i*: dc
Input type input V1: differential
Input type input V2: differential
Outer conductor type input V1: grounded*

*The preferred setting for this experimental configuration, "floating," could not be used when the furnace was running above about 60 pct power (*i.e.*, at temperatures above about 1400 °C); the "grounded" setting had to be used to avoid input and generator overload errors on the 1260 FRA due to pick up of intense 60 Hz noise from the heater.

Outer conductor type input V2: grounded

B. *Experiment*

Sweep type: log
Log increment type: steps per decade
Log increment value: 33
Initial sweep frequency: 350 kHz
Final sweep frequency: 1 kHz
Bias current: 0
Monitor: off
Generator current (mA): 40 mA
Display axes: triple plot

REFERENCES

1. D.R. Sadoway: U.S. Patent No. 5,185,068, Feb. 9, 1993.
2. D.R. Sadoway: *J. Mater. Res.*, 1995, vol. 10, pp. 487-92.
3. *Phase Diagrams for Ceramists*, E.M. Levin, C.R. Robbins, and H.F. McMurdie, eds., American Ceramic Society, Columbus, OH, 1964, p. 210.
4. D.R. Sadoway, K.G. Rhoads, N.A. Fried, and S.L. Schiefelbein: U.S. Patent No. 5,489,849, Feb. 6, 1996.
5. S.L. Schiefelbein: Ph.D. Thesis, Massachusetts Institute of Technology, Cambridge, MA, 1996.
6. Y.C. Wu, W.F. Koch, W.J. Hamer, and R.L. Kay: *J. Sol. Chem.*, 1987, vol. 16, pp. 985-97.
7. Y.C. Wu and W.F. Koch: *J. Solution Chem.*, 1991, vol. 20, pp. 391-401.
8. K.C. Mills: *Iron Steel Inst. Jpn. Int.*, 1993, vol. 33, pp. 148-55.
9. K.C. Mills and B.J. Keene: *Int. Mater. Rev.*, 1987, vol. 32, pp. 1-120.
10. P.L. Lin and A.D. Pelton: *Metall. Trans. B*, 1975, vol. 10B, pp. 667-75.
11. C. Bodsworth: *Physical Chemistry of Iron and Steel Manufacture*, Longmans Green and Co., Ltd., London, 1963.
12. W.D. Kingery, H.K. Bowen, and D.R. Uhlmann: *Introduction to Ceramics*, John Wiley & Sons, New York, NY, 1976.
13. J. O'M. Bockris and A.K.N. Reddy: *Modern Electrochemistry*, Plenum Publishing Corp., New York, NY, 1973.
14. M. Kawahara, Y. Ozima, K. Morinaga, and T. Yanagase: *J. Jpn. Inst. Met.*, 1978, vol. 42, pp. 618-23.
15. R.H. Aiken: U.S. Patent No. 816,142, Mar. 27, 1906.
16. M.T. Simnad, G. Derge, and I. George: *J. Met.*, 1954, vol. 6, pp. 1386-90.
17. W.R. Dickson and E.B. Dismukes: *Trans. AIME*, 1962, vol. 224, pp. 505-11.
18. A.K. Kir'yanov and O.A. Esin: *Tr. Inst. Metall., Akad. Nauk S.S.S.R., Ural. Fil.*, 1960, No. 5, pp. 87-92.
19. P.M. Shurygin and O.A. Esin: *Fiziko-Khimicheskie Osnovy*

Proizvodstva Stali, Trudy Konferentsii po Fiziko-Khimicheskim Osnovam Proizvodstva Stali, Moscow, Jan. 24–29, 1955, 1957, pp. 464-68.

20. V.V. Stender: *Vestnik Akad. Nauk Kazakh. S.S.R.*, 1960, No. 10, pp. 66-70.
21. A. Adachi and K. Ogino: *Denki Kagaku*, 1964, vol. 32, pp. 145-49.
22. M.T. Simnad and G. Derge: *J. Chem. Phys.*, 1953, vol. 21, pp. 933-34.
23. J.W. Tomlinson and H. Inouye: *J. Chem. Phys.*, 1952, vol. 20, p. 193.
24. D.A. Dukelow and G. Derge: *Trans. AIME*, 1960, vol. 218, pp. 136-41.
25. M. Zahn, Electromagnetic Field Theory: A Problem Solving Approach, John Wiley & Sons, New York, 1979.